Application Prospects of MgB_2 in View of Its Basic Properties

Michael Eisterer and Harald W. Weber

***Abstract*—Seven years after the discovery of superconductivity in magnesium diboride, the fundamental superconducting properties of this compound are well known and the peculiar current transport in polycrystalline materials is essentially understood. Based on this knowledge the ultimate performance of wires or tapes at high magnetic fields will be predicted and compared to state-of-the-art materials and to other superconductors. The key parameter for high field applications is the upper critical field, which can be strongly enhanced by impurity scattering. This fundamental property might be further optimized in bulk materials, since higher values were reported for thin films. The MgB_2 grains are usually very small, if prepared by the in-situ technique. The resulting high density of grain boundaries leads to strong pinning, close to the theoretical limit. On the other hand, the connectivity between the grains is still rather poor and strongly reduces the achievable critical currents, thus leaving room for further improvements.**

***Index Terms*—Connectivity, critical currents, magnesium diboride, upper critical field.**

I. Introduction

THE CRITICAL current density J_c is the most important quantity for power applications. Its magnitude is given by the pinning strength and its field dependence is determined by the density and morphology of pins and by the upper critical field. At low magnetic fields, J_c can be around 15–20% of the depairing current density J_d in a type II superconductor with optimized pinning [1]. This limit is obtained from the balance of the maximum force a single pin can exert on a flux line and the Lorentz force acting on this ideally pinned vortex. As long as the density of such strong pins is significantly higher than the density of vortices, J_c can meet this theoretical limit. At higher magnetic fields, not all flux lines are perfectly pinned anymore and J_c starts to decrease. This is illustrated in Fig. 1 (open squares). The low field J_c is given by the pinning force of an individual pin or, more precisely, by the sum of the forces of all pins acting on the same flux line. The field B_{sv}, where the plateau ends, is determined by the pin density. At higher fields, the field dependence is given by the morphology of the defects [2] and by the upper critical field B_{c2}. For the sake of simplicity, the critical currents are assumed to reach zero at B_{c2}, since thermal fluctuations are unimportant in MgB_2 [3].

Manuscript received August 17, 2008. First published June 05, 2009; current version published July 15, 2009.

The authors are with the Atomic Institute of the Austrian Universities, TU Vienna, 1020 Vienna, Austria (e-mail: eisterer@ati.ac.at; weber@ati.ac.at).

Color versions of one or more of the figures in this paper are available online at http://ieeexplore.ieee.org.

Digital Object Identifier 10.1109/TASC.2009.2019538

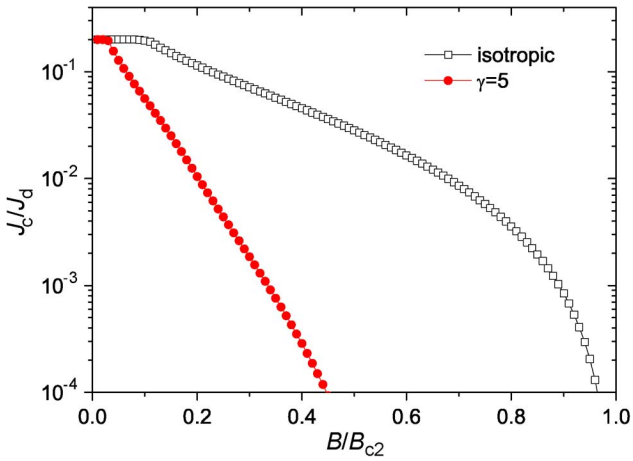

Fig. 1. Influence of the upper critical field anisotropy on the critical current densities. The field and current densities are normalized by the upper critical field and the depairing current density, respectively. Calculations are based on grain boundary pinning.

The field dependence of the critical current densities plotted in Fig. 1 is predicted for grain boundary pinning [2] which is most important in MgB_2 [4], [5] and will be considered in the following. J_c is given by

$$J_c(B) = A_{con}\eta_{pin}J_d\frac{\left(1-\frac{B}{B_{c2}}\right)^2}{\sqrt{B}} \quad (1)$$

for fields above B_{sv}. A_{con} is one in the ideal case and describes the suppression of the current density due to a reduction of the effective cross section resulting from porosity, secondary phases or badly connected grains [6]. η_{pin} characterizes the pinning efficiency. A_{con} and η_{pin} are not intrinsic to a certain material but given by the actual pinning centers or microstructure. With optimized values for these extrinsic parameter, $J_c(B)$ is entirely determined by the two intrinsic parameters J_d and B_{c2}. The depairing current density scales the y-axis in Fig. 1, the upper critical field scales the x-axis. These fundamental parameters of MgB_2 are compared to those of other technologically important superconductors in Table I. All values refer to zero temperature. The depairing current density in MgB_2 is much higher than in NbTi and even comparable to that in high temperature superconductors. Only Nb_3Sn has a significantly larger depairing current density. Because of the two band nature of superconductivity in MgB_2 and the suppression of the π gap at high magnetic fields, J_d slightly decreases with magnetic field (to about 1.3×10^{12} A m^2 [5]).

The upper critical field at 0 K is rather low in clean MgB_2 ($\sim$14 T), comparable to NbTi. Note that the given value refers to

TABLE I
DEPAIRING CURRENT DENSITIES AND UPPER CRITICAL FIELDS OF VARIOUS SUPERCONDUCTORS AT ZERO TEMPERATURE.

	MgB_2	NbTi	Nb_3Sn	HTS
$J_d(10^{12}\,A\,m^{-2})$	2	0.4	7	3
B_{c2}(T)	14-70 ($H\|ab$)	15	30	150 ($H\|c$)

the apparent B_{c2} in polycrystalline MgB_2, which corresponds to B_{c2}^{ab} (field parallel to the boron planes). Disorder enhances the upper critical field significantly, as discussed in Section III, and values of up to 74 T were reported [7].

These two fundamental parameters (J_d, B_{c2}) indicate that MgB_2 is a promising high field conductor. Unfortunately, the anisotropic magnetic properties of magnesium diboride complicate the current transport and reduce the critical currents at high magnetic fields significantly.

II. UPPER CRITICAL FIELD ANISOTROPY

The upper critical field anisotropy, γ, changes the field dependence of the critical current density [8] and of the corresponding volume pinning force [9] drastically. This is illustrated in Fig. 1. The solid circles represent J_c in a polycrystalline material with an anisotropy factor of 5, which is representative for clean MgB_2. The field, $B_{\rho=0}$, where the critical currents reach zero, decreases by a factor of $((\gamma^2-1)p_c^2+1)^{-1/2}$ [10] compared to the corresponding isotropic material and the field dependence of J_c is enhanced. The percolation threshold p_c denotes the minimum fraction of superconducting material for a continuous current path and is expected to be 0.2 to 0.3 [8]. In the following $p_c = 0.25$ is assumed, leading to a reduction of $B_{\rho=0}$ to $0.63B_{c2}$ (for $\gamma = 5$). All calculations are based on the model proposed in [8], but with the anisotropic scaling approach [11], as described in [9].

The anisotropy is the third intrinsic parameter which influences the critical currents in MgB_2.

III. DISORDER IMPROVES THE HIGH FIELD PROPERTIES

The low upper critical field and the high anisotropy of clean MgB_2 restrict high currents to low magnetic fields (cf. Fig. 1). Impurity scattering helps to solve this problem by enhancing the upper critical field and reducing its anisotropy at the expense of a slight decrease in T_c. This reduction of the transition temperature is caused by interband scattering between the σ- and the π-bands and by intraband scattering within the σ-bands. Intraband scattering can reduce T_c only in anisotropic superconductors or, indirectly, via a reduction of the density of states (DOS) at the Fermi level, as observed in MgB_2 [12]. Since intraband scattering in the σ-bands is also responsible for the increase in the upper critical field, a decrease in T_c is inherent in the enhancement of B_{c2} by impurity scattering. The additional amount of interband scattering potentially depends on the actual defect structure and leads to sample to sample variations. The same holds for charge doping (e.g. by carbon or aluminum), which also reduces the DOS [13]–[15]. Nevertheless, a remarkable similarity in resistivity, transition temperature and upper critical field was found in samples with a totally different defect structure (as grown defects, SiC doping, neutron induced defects) [16]. Thus, the transition temperature turns out to be a useful disorder parameter.

The beneficial effect of the decrease of the mean free path of the charge carriers has to compete with the decrease of T_c leading to a maximum of B_{c2} as a function of the transition temperature. B_{c2} in most samples with a transition temperature above 33 K ($B_{c2} <\sim 40$ T) reasonably follows the relation [5]

$$B_{c2}(T_c) = 13.8\left(t_c^2 + 16.7t_c(1-t_c)\right)\ \mathrm{T} \tag{2}$$

with $t_c := (T_c/T_c^{clean})$ and $T_c^{clean} = 39.43$ K. B_{c2} of samples with a smaller transition temperature normally deviates from this relation, as demonstrated by irradiation [17]–[19] or doping [20]–[22] experiments. Only carbon doped fibers [23] follow (2) at lower transition temperatures, with $B_{c2} = 55$ T at $T_c = 28$ T, which is close to the predicted maximum of about 60 T at $T_c \sim 21$ T. The doped fibers and results obtained on thin films, where upper critical fields of up to 74 T were found [7], suggest that the highest reported values in bulk samples (around 40 T) are not a fundamental limit and that the deviations from (2) at low transition temperatures are caused by an additional not inherent effect (e.g. strong interband scattering). However, the validity of (2) down to low transition temperatures will be assumed in the following, which is optimistic, since the maximum B_{c2} at around 21 K was not yet achieved in bulk samples. On the other hand, many reports claim slightly higher upper critical fields at a certain transition temperature (>33 K) than predicted by (2), which reflects the *average* behavior of data extracted from literature [5]. Ideal intraband scattering centers inducing only a minimum fraction of interband scattering could lead to higher values of the upper critical field at a given transition temperature than predicted by (2).

A further benefit of impurity scattering is the reduction of the upper critical field anisotropy [19] which is also strongly correlated with the reduction of T_c [19], [5]:

$$\gamma(T_c) = \frac{t_c^2 + 16.7t_c(1-t_c)}{3.88 - 3.724t_c}. \tag{3}$$

The depairing current density is expected to decrease by the introduction of disorder, since $J_d \propto B_c^2\xi \propto T_c^2/\sqrt{B_{c2}}$. Both, the reduction of T_c and the enhancement of B_{c2}, decrease J_d. The estimate $T_c \propto B_c$ is based on the proportionality between the thermodynamic critical field, B_c, and the energy gap, which was shown to scale with T_c in the σ-band [24]–[26]. With this dependence of J_d on T_c and B_{c2} and with the dependencies of B_{c2} and γ according to (2) and (3), the critical current density (at fixed field and temperature) is a unique function of the transition temperature for a given $A_{con}\eta_{pin}$. Fig. 2 compares the field dependence of the critical currents in clean ($T_c = 39$ T) and disordered ($T_c = 34$ K) MgB_2.

IV. OPTIMIZATION OF THE MATERIAL PROPERTIES

Since the improvements in B_{c2} and γ induced by impurity scattering have to compete with the reduction of J_d and T_c, an optimal amount of disorder maximizes the critical current density at a certain field and temperature. This is illustrated in Fig. 3 for 8 T and 4.2 K.

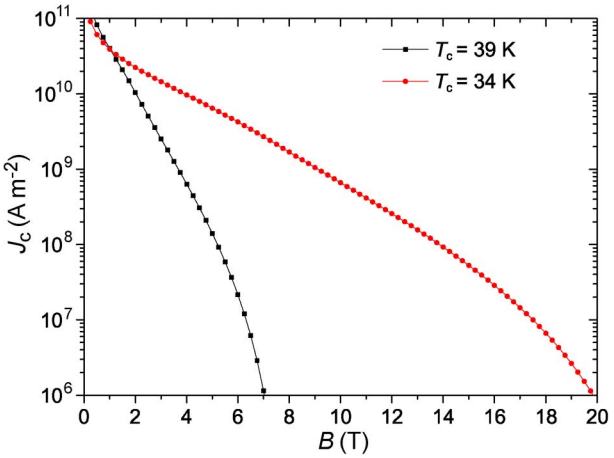

Fig. 2. Influence of disorder on the critical current densities. T_c serves as disorder parameter.

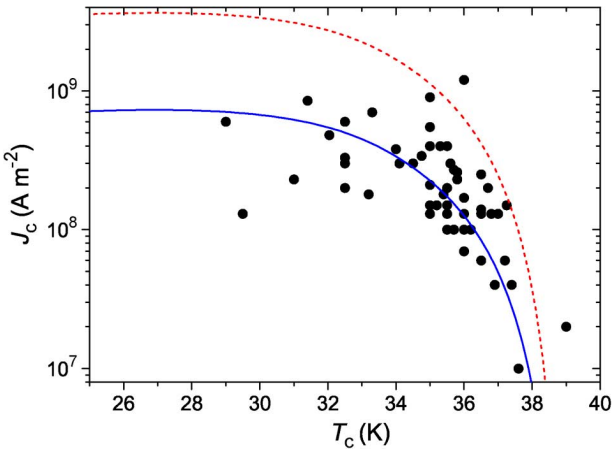

Fig. 3. Critical current densities at 4.2 K and 8 T as a function of the transition temperature. Experimental data are shown for comparison (solid circles). They were extracted from literature in [5] and a view more recent data were added in this plot [27]–[38].

The only free parameter left is the product of $A_{\rm con}$ and $\eta_{\rm pin}$, which is temperature independent and can be chosen to fit the experimental data (solid line in Fig. 3). The overall agreement between the experimental data and the predicted behavior is quite good, given the fact that $A_{\rm con}$ and $\eta_{\rm pin}$ are expected to vary from sample to sample. The main increase of the high field J_c was achieved by the introduction of scattering centers in the last few years, which decreased T_c to about 32–35 K. A further decrease of T_c seems to be less beneficial, although the predicted maximum of J_c is at around 27 K.

It is interesting to compare the experimental data to the expected maximum of $A_{\rm con}\eta_{\rm pin}$. $A_{\rm con}$ is one in the ideal case, but it is difficult to estimate the theoretical limit of $\eta_{\rm pin}$. As pointed out in the introduction, the maximum low field J_c is expected to be around $0.2J_{\rm d}$. Due to the divergence of J_c in (1) for $B \to 0$, $A_{\rm con}\eta_{\rm pin}$ cannot be determined from the self field J_c alone. The field, where the low field plateau ends, is crucial and depends on the density of strong pins. It should be pointed out that the low field behavior of the critical currents is difficult to determine, since the self field of the currents becomes quite large at $0.2J_{\rm d} \approx 4 \times 10^{11}$ A m^{-2}. Approximately 1 T can be estimated as the maximum self field for a 400 nm thick film (only weakly dependent on its lateral dimensions) and 200 T (!) for a cube of 1 mm^3. The latter is of course totally unrealistic, since the self field strongly reduces the currents leading in turn immediately to much smaller self fields. Nevertheless, the self field remains quite large in bulk samples and impedes the assessment of J_c at low fields. Self field current densities of around 4×10^{11} A m^{-2} were reported in thin films [39] indicating the presence of optimal pinning centers. J_c is usually about one order of magnitude lower at 1 T [5] which might result from a comparatively low density of such pins. The mean distance between two pins should be significantly smaller than the lattice parameter of the flux line lattice which is about 44 nm at 1 T. However, from $J_c(1\ {\rm T}, 4.2\ {\rm K}) = 4 \times 10^{10}$ A m^{-2} one can estimate $A_{\rm con}\eta_{\rm pin}$ to be about 0.018 T$^{0.5}$. The dotted line in Fig. 3 is based on this value, which is about 5 times larger than the average experimental one in polycrystalline materials (solid line). It is in principle not possible to distinguish whether pinning is less efficient in such materials or whether the connectivity is reduced in comparison to thin films. The typical low densities of the filaments and the presence of secondary phases favor the latter [5], which is supported by electron microscopy [40]. However, $A_{\rm con}\eta_{\rm pin} = 0.018$ T$^{0.5}$ is used in the following, which is not a theoretical limit, but corresponds to the highest reported critical current densities in well connected films. Nanometer sized grains were found not only in these "high J_c" films, but also in bulks, wires or tapes. It is interesting to note that two experimental points [35], [41], lie *above* this "optimal" performance. Both samples were prepared by an internal magnesium diffusion process. (The data point at 39 K extracted from [41] was slightly extrapolated from lower field values. T_c is given only approximately (≈36 T) in [35].) This gives hope that this prediction is still too pessimistic, although it might be simply a consequence of a slight overestimation of T_c because of material inhomogeneity. In this case the grains or regions of the sample which determine the onset of the superconducting transition are not responsible for the high field behavior at low temperatures [5].

The optimal amount of scattering centers depends on the operating conditions. The potentially highest J_c at each field was calculated and is presented in Fig. 4 (open circles). A clean material with optimum T_c is favorable at low fields. With increasing field, disorder should increase and the optimum T_c is predicted to be about 21 K for magnetic fields above about 20 T. This implicitly assumes a B_{c2} of 47 T at 4.2 K [(2) and (4)], which was only realized in fibers [23] or films [7] so far (although at higher transition temperatures). If B_{c2} cannot be improved beyond 40 T, the optimum high field J_c is expected to be similar to that of the "34 K sample" in Fig. 2. ($A_{\rm con}\eta_{\rm pin} = 0.018$ T$^{0.5}$ was assumed also in these calculations.)

Typical magnet applications require a current density J_c of about 10^9 A m^{-2}, for large magnets (e.g. in fusion power plants) 2×10^8 A m^{-2} might be acceptable. At 4.2 K, these criteria are met at 14 T and 21 T, respectively.

MgB_2 could also be used at higher temperatures, thus the temperature dependence of the "application fields" was calculated. The results are shown in Fig. 5. The depairing current density was assumed to decrease with temperature as $J_{\rm d}(T) \propto$

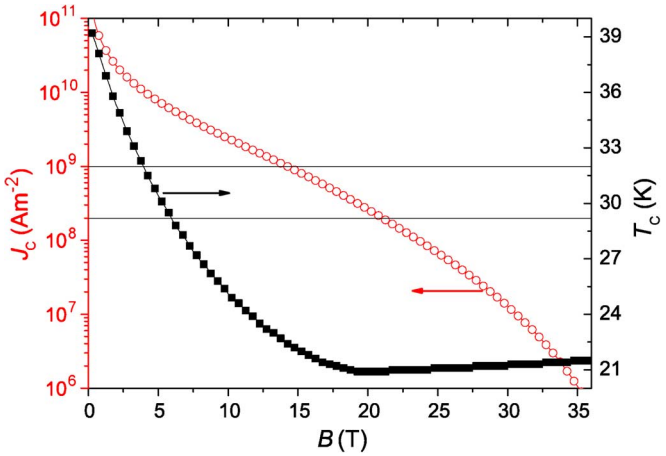

Fig. 4. Optimum critical current densities at 4.2 K (open circles) and corresponding transition temperatures (solid squares). Horizontal lines indicate typical application criteria.

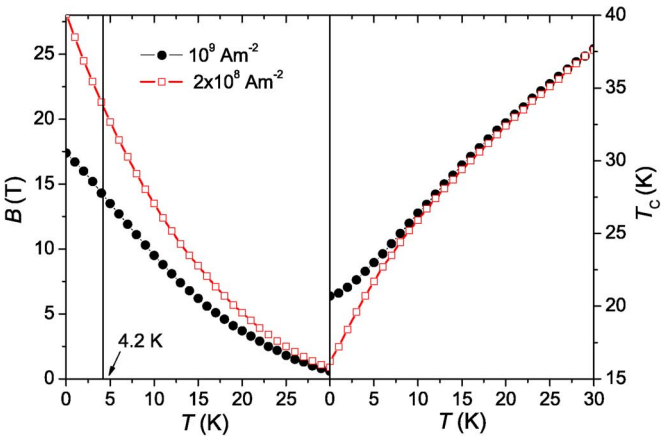

Fig. 5. Left panel: Fields and temperatures where the optimum J_c is 10^9 A m^{-2} (solid circles) and 2×10^8 A m^{-2} (open squares). Right panel: Corresponding transition temperature.

$B_c(T)^2\xi(T) \propto (1-(T/T_c)^2)^2/\sqrt{B_{c2}(T)}$. The upper critical field was modeled by

$$B_{c2}(T) = B_{c2}(0)\,(1 - T/(T_c - 4\,\mathrm{K}))\,. \tag{4}$$

A linear dependence of B_{c2} on temperature is often observed in MgB_2 at intermediate temperatures. This linear behavior does not extrapolate to zero at T_c, but at a slightly smaller temperature, therefore, 4 K are subtracted from T_c in the denominator in (4). The usually observed tail in $B_{c2}(T)$ near T_c is neglected, since the temperature range near T_c is unimportant for applications. Note that the experimental data of $B_{c2}(0)$, on which (2) is based, were often obtained from a linear extrapolation of $B_{c2}(T)$ at intermediate temperatures, which makes the present estimation of $B_{c2}(T)$ consistent with these data.

The critical current density is above 10^9 A m^{-2} up to about 3.7 T at 20 K and above 2×10^8 A m^{-2} up to about 5 T (Fig. 5). These values should not be taken too literally, because of the numerous assumptions.

The optimum transition temperature increases with the application temperature and depends only weakly on the application criterion. Only at low temperatures significant differences between the 10^9 A m^{-2} and the 2×10^8 A m^{-2} curves are found (right panel in Fig. 5). The optimum transition temperature at liquid helium temperature is still much lower than in state-of-the art materials (if (2) could be realized). At 20 K the optimum T_c is predicted to be around 32.5 K which is comparable to today's materials. Thus, a further increase of impurity scattering is not expected to improve the properties at 20 K. This can be realized only by improving the connectivity or pinning.

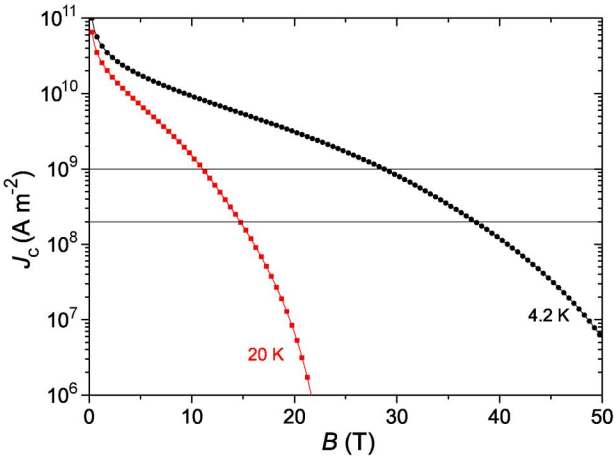

Fig. 6. A more optimistic scenario: Calculations are based on the best thin film performance reported so far.

Last we consider an even more optimistic scenario based on the best demonstrated thin film performance. An upper critical field of around 63 T at 4.2 K with an anisotropy of about 1.85 was found in a thin film with $T_c = 35$ T [7]. B_{c2} of the same film was 27 T at 20 K with an anisotropy of about 2.2. With these parameters and $A_{con}\eta_{pin}$ as above (demonstrated at *other* films), $J_c(B)$ was calculated, assuming the same dependence of J_d on T, T_c and B_{c2}. The results are shown in Fig. 6. The application field is shifted to around 30 T at 4.2 K and to about 13 T at 20 K.

V. Conclusions

The optimum high field performance of MgB_2 was calculated based on its intrinsic parameters, namely upper critical field, depairing current density, anisotropy and transition temperature. It turns out that the optimal amount of impurity scattering depends on the operation conditions (field and temperature). The upper critical field and the anisotropy were extrapolated from literature data, which only reflect an average behavior. Therefore, further improvements can be expected by optimization of the inter-/intraband scattering rates. This is encouraged by results obtained on thin films. Other promising ways of enhancing the critical currents are an improvement in the connectivity between the grains and of the MgB_2 density in wires or tapes. At low temperatures, MgB_2 has certainly the potential to beat the high field performance of NbTi and even to approach that of Nb_3Sn. At 20 K intraband scattering seems to be nearly optimized in today's state-of-the-art samples.

If the high upper critical fields observed in dirty thin films with rather high transition temperatures could be obtained also in polycrystalline MgB_2, the high field performance would significantly improve.

REFERENCES

[1] D. H. Arcos and M. N. Kunchur, "Suppressed flux motion in magnesium diboride films," *Phys. Rev. B.*, vol. 71, p. 184516, 2005.

[2] D. Dew-Hughes, "Flux pinning mechanisms in type II superconductors," *Phil. Mag.*, vol. 30, p. 293, 1974.

[3] A. E. Koshelev, A. A. Varlamov, and V. M. Vinokur, "Theory of fluctuations in a two-band superconductor: MgB_2," *Phys. Rev. B*, vol. 72, p. 064523, 2005.

[4] E. Martínez, P. Mikheenko, M. Martínez-López, A. Millán, A. Bevan, and J. S. Abell, "Flux pinning force in bulk MgB_2 with variable grain size," *Phys. Rev. B*, vol. 75, p. 134515, 2007.

[5] M. Eisterer, "Magnetic properties and critical currents of MgB_2," *Supercond. Sci. Technol.*, vol. 20, p. R47, 2007.

[6] J. M. Rowell, "The widely variable resistivity of MgB_2 samples," *Supercond. Sci. Technol.*, vol. 16, p. R17, 2003.

[7] V. Braccini *et al.*, "High-field superconductivity in alloyed MgB_2 thin films," *Phys. Rev. B*, vol. 71, p. 012504, 2005.

[8] M. Eisterer, M. Zehetmayer, and H. W. Weber, "Current percolation and anisotropy in polycrystalline MgB_2," *Phys. Rev. Lett.*, vol. 90, no. 24, p. 247002, Jun. 2003.

[9] M. Eisterer, "Calculation of the volume pinning force in MgB_2 superconductors," *Phys. Rev. B*, vol. 77, p. 144524, 2008.

[10] M. Eisterer, C. Krutzler, and H. W. Weber, "Influence of the upper critical-field anisotropy on the transport properties of polycrystalline MgB_2," *J. Appl. Phys.*, vol. 98, p. 033906, 2005.

[11] G. Blatter, V. B. Geshkenbein, and A. I. Larkin, "From isotropic to anisotropic superconductors: A scaling approach," *Phys. Rev. Lett.*, vol. 68, p. 875, 1992.

[12] M. Putti, P. Brotto, M. Monni, E. Galleani, A. Sanna, and S. Massidda, "Intraband vs. interband scattering rate effects in neutron irradiated MgB_2," *Eurohys. Lett.*, vol. 77, p. 57005, 2007.

[13] O. de la Peña, A. Aguayo, and R. de Coss, "Effects of al doping on the structural and electronic properties of $Mg_{1-x}Al_xB_2$," *Phys. Rev. B*, vol. 66, no. 1, p. 012511, Jul. 2002.

[14] G. A. Ummarino, D. Daghero, R. S. Gonnelli, and A. H. Moudden, "Carbon substitutions in MgB_2 within the two-band Eliashberg theory," *Phys. Rev. B*, vol. 71, p. 134511, 2005.

[15] J. Jens Kortus, O. V. Dolgov, R. K. Kremer, and A. A. Golubov, "Band filling and interband scattering effects in MgB_2: Carbon versus aluminum doping," *Phys. Rev. Lett.*, vol. 94, p. 027002, 2005.

[16] M. Eisterer, R. Müller, R. Schöppl, H. W. Weber, S. Soltanian, and S. X. Dou, "Universal influence of disorder on MgB_2 wires," *Supercond. Sci. Technol.*, vol. 20, p. 117, 2007.

[17] R. Gandikota *et al.*, "Effect of damage by 2 MeV He ions and annealing on H_{c2} in MgB_2 thin films," *Appl. Phys. Lett.*, vol. 87, p. 072507, 2005.

[18] C. Tarantini *et al.*, "Effects of neutron irradiation on polycrystalline $Mg^{11}B_2$," *Phys. Rev. B*, vol. 73, p. 134518, 2006.

[19] C. Krutzler, M. Zehetmayer, M. Eisterer, H. W. Weber, N. D. Zhigadlo, and J. Karpinski, "Comparative study of neutron irradiation and carbon doping in MgB_2 single crystals," *Phys. Rev. B*, vol. 75, p. 224510, 2007.

[20] R. H. T. Wilke, S. L. Bud'ko, P. C. Canfield, D. K. Finnemore, R. J. Suplinskas, and S. T. Hannahs, "Systematic effects of carbon doping on the superconducting properties of $Mg(B_{1-x}C_x)_2$," *Phys. Rev. Lett.*, vol. 92, p. 217003, 2004.

[21] M. Angst, S. L. Bud'ko, R. H. T. Wilke, and P. C. Canfield, "Difference between Al and C doping in anisotropic upper critical field development in MgB_2," *Phys. Rev. B.*, vol. 71, p. 144512, 2005.

[22] C. Krutzler, M. Zehetmayer, M. Eisterer, H. W. Weber, N. D. Zhigadlo, J. Karpinski, and A. Wisniewski, "Anisotropic reversible mixed-state properties of superconducting carbon-doped $Mg(B_{1-x}C_x)_2$ single crystals," *Phys. Rev. B*, vol. 74, p. 144511, 2006.

[23] V. Ferrando *et al.*, "High upper critical field and irreversibility field in MgB_2 coated-conductor fibers," *Appl. Phys. Lett.*, vol. 87, p. 252509, 2005.

[24] R. S. Gonnelli, D. Daghero, A. Calzolari, G. A. Ummarino, V. Dellarocca, V. A. Stepanov, S. M. Kazakov, N. Zhigadlo, and J. Karpinski, "Evidence for single-gap superconductivity in $Mg(B_{1-x}C_x)_2$ single crystals with $x = 0.132$ from point-contact spectroscopy," *Phys. Rev. B*, vol. 71, p. 060503(R), 2005.

[25] A. J. Zambano, A. R. Moodenbaugh, and L. D. Cooley, "Effects of different reactions on composition homogeneity and superconducting properties of Al-doped MgB_2," *Supercond. Sci. Technol.*, vol. 18, p. 1411, 2005.

[26] M. Putti, M. Affronte, C. Ferdeghini, P. Manfrinetti, C. Tarantini, and E. Lehmann, "Observation of the crossover from two-gap to single-gap superconductivity through specific heat measurements in neutron-irradiated MgB_2," *Phys. Rev. Lett.*, vol. 96, p. 077003, 2006.

[27] M. Herrmann, W. Haessler, C. Rodig, W. Gruner, B. Holzapfel, and L. Schultz, "Touching the properties of NbTi by carbon doped tapes with mechanically alloyed MgB_2," *Appl. Phys. Lett.*, vol. 91, p. 082507, 2007.

[28] M. Herrmann, W. Häßler, C. Mickel, W. Gruner, B. Holzapfel, and L. Schultz, "The effect of reactive nanostructured carbon on the superconducting properties of mechanically alloyed MgB_2," *Supercond. Sci. Technol.*, vol. 20, p. 1108, 2007.

[29] Y. Hishinuma, A. Kikuchi, and T. Takeuchi, "Superconducting properties and microstructure of MgB_2 wires synthesized with a low-temperature diffusion process," *Supercond. Sci. Technol.*, vol. 20, p. 1178, 2007.

[30] J. H. Kim, S. X. Dou, D. Q. Shi, M. Rindfleisch, and M. Tomsic, "Study of mgo formation and structural defects in in situ processed MgB_2/Fe wires," *Supercond. Sci. Technol.*, vol. 20, p. 1026, 2007.

[31] P. Kováč, I. Hušek, T. Melišek, and T. Holúbek, "Properties of stabilized MgB_2 composite wire with Ti barrier," *Supercond. Sci. Technol.*, vol. 20, p. 771, 2007.

[32] B. J. Senkowicz, A. Polyanskii, R. J. Mungall, Y. Zhu, J. E. Giencke, P. M. Voyles, C. B. Eom, E. E. Hellstrom, and D. C. Larbalestier, "Understanding the route to high critical current density in mechanically alloyed $Mg(B_{1-x}C_x)_2$," *Supercond. Sci. Technol.*, vol. 20, p. 035009, 2007.

[33] D. Wang, Y. Ma, Z. Yu, Z. Gao, Z. Xianping, K. Watanabe, and E. Mossang, "Strong influence of precursor powder on the critical current density of Fe-sheathed MgB_2 tapes," *Supercond. Sci. Technol.*, vol. 20, p. 574, 2007.

[34] H. Fujii, K. Togano, and K. Ozawa, "Effects of both addition and chemical treatment of SiC nanoparticles on the grain coupling and critical current density in ex situ processed MgB_2 tapes," *Supercond. Sci. Technol.*, vol. 21, p. 015002, 2008.

[35] J. M. Hur, K. Togano, A. Matsumoto, H. Kumakura, H. Wada, and K. Kimura, "Fabrication of high-performance MgB_2 wires by an internal Mg diffusion process," *Supercond. Sci. Technol.*, vol. 21, p. 032001, 2008.

[36] B. J. Senkowicz, R. J. Mungall, Y. Zhu, J. Jiang, P. M. Voyles, E. E. Hellstrom, and D. C. Larbalestier, "Nanoscale grains, high irreversibility field and large critical current density as a function of high-energy ball milling time in C-doped magnesium diboride," *Supercond. Sci. Technol.*, vol. 21, p. 035009, 2008.

[37] O. V. Shcherbakova, A. V. Pan, J. L. Wang, A. V. Shcherbakov, S. X. Dou, D. Wexler, E. Babić, M. Jerčinović, and O. Husnjak, "Sugar as an optimal carbon source for the enhanced performance of MgB_2 superconductors at high magnetic fields," *Supercond. Sci. Technol.*, vol. 21, p. 015005, 2008.

[38] X. Zhang, Y. Ma, Z. Gao, D. Wang, L. Wang, W. Liu, and C. Wang, "Strongly enhanced current-carrying performance in MgB_2 tape conductors by C_{60} doping," *J. Appl. Phys.*, vol. 103, p. 103915, 2008.

[39] H.-J. Kim, W. N. Kang, E.-M. Choi, M.-S. Kim, K. H. P. Kim, and S.-I. Lee, "High current-carrying capability in c-axis-oriented superconducting MgB_2 thin films," *Phys. Rev. Lett.*, vol. 87, no. 8, p. 087002, Aug. 2001.

[40] B. Birajdar, N. Peranio, and O. Eibl, "Quantitative electron microscopy and spectroscopy of MgB_2 wires and tapes," *Supercond. Sci. Technol.*, vol. 21, p. 073001, 2008.

[41] G. Giunchi, S. Ceresara, G. Ripamonti, A. Di Zenobio, S. Rossi, S. Chiarelli, M. Spadoni, R. Wesche, and P. L. Bruzzone, "High performance new MgB_2 superconducting hollow wires," *Supercond. Sci. Technol.*, vol. 16, p. 285, 2003.